THE JOURNAL OF PHYSICAL CHEMISTRY C

Article

Cite This: J. Phys. Chem. C 2019, 123, 18502−18507

pubs.acs.org/JPCC

Diffusion Mechanisms for Ions over Hydroxylated Surfaces: Cu on γ-Al_2O_3

Manuel J. Louwerse,*[†] Marco Piccinini,[‡] and Krijn P. de Jong[†]

[†]Inorganic Chemistry and Catalysis, Debye Institute for Nanomaterials Science, Utrecht University, 3584 CG Utrecht, The Netherlands

[‡]Research Technology & Engineering, Inovyn Belgium, Rue Solvay 39, 5190 Jemeppe sur Sambre, Belgium

Supporting Information

ABSTRACT: The energies involved in the diffusion of Cu^{2+} and Cu^{+} over hydroxylated γ-alumina were modeled with density functional theory using explorative molecular dynamics. This is the first time that the mechanism for diffusion of ions over hydroxylated surfaces is studied. It is found that the crucial requirement for feasible activation energies for ion diffusion is the prevention of charge separation. This can be realized either by counterion codiffusion or proton contradiffusion. Furthermore, the effects of the cation valency, hydroxylation level, and nature of the counterions were studied and general trends for diffusing cations on hydroxylated surfaces were postulated. At full hydroxylation, all charge compensation is performed by proton contradiffusion, while at intermediate hydroxylation levels, a combination of proton contradiffusion and counterion codiffusion occurs. Finally, energy barriers for codiffusion are related to the bonding strength of the counterions to the surface, which depends on the counterion and the hydroxylation level.

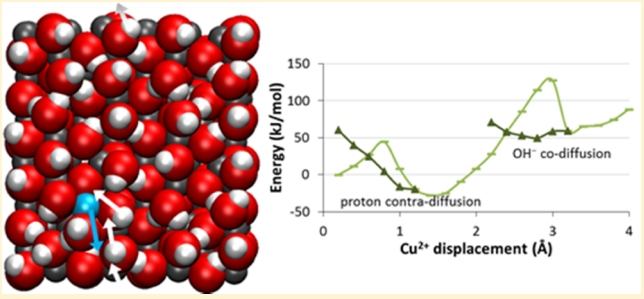

INTRODUCTION

Diffusion of molecules and atoms is important in many branches of chemistry. Obviously, for chemical reactions in gaseous or liquid media, molecules need to diffuse to meet each other.[1] Also in solid-state chemistry, both for bulk and nanomaterials, diffusion processes are often critical processes: to form the desired structures, atoms need to arrive at the correct locations.[2] Concurrently, structural changes due to long lifetimes or intense material usage can cause structural attenuation or functional deactivation, for instance through segregation or sintering.[3,4] All this is driven by atomic diffusion at the Ångstrom scale, with molecular modeling as an invaluable tool for understanding these fundamental processes to the utmost detail.

Focusing on the diffusion of metal atoms and ions over surfaces, the literature starts with the study of metal adatoms on metal surfaces.[5−8] Experiments show that there are in fact two possible mechanisms for adatom diffusion: straightforward hopping across the surface and exchanging with surface atoms, which yields a net diffusion. Molecular modeling gives the same two mechanisms, with the added opportunity to study what determines the preferred pathway.[9−14]

As a next step, the focus shifted to metal atoms and clusters on oxide surfaces, both for modeling[15−19] and experimental studies.[20,21] On pristine surfaces, several different diffusion mechanisms were observed, where clusters would either slide, roll, or walk over the oxide surface.[15,16] Moreover, when defects are present in the oxide surface, a concerted diffusion of metal clusters and support defects is possible.[17] However, for several oxides, the surface usually is not pristine since hydroxyl groups will be present at the surface, at least for any practical application where the metal is deposited from an aqueous phase. Examples are α-Al_2O_3,[22,23] γ-Al_2O_3,[24] and SiO_2.[25] Obviously, the hydroxylation layer on these oxides strongly influences the diffusion behavior of adsorbed metal atoms, in most cases leading to an increase of the diffusion barriers.[26−29] Experimentally, this was studied by investigating the sintering behavior of originally isolated adatoms on such surfaces, also showing that in most cases sintering is slower when a surface is hydroxylated.[26,30,31] For catalysis, such knowledge of determining factors for particle growth during application is very important.

However, while model systems may be prepared by deposition of atoms from the gas phase, practical catalysts are usually prepared with wet preparation methods from solutions of their salts.[32] This means that in the former case deposited clusters and nanoparticles may consist of neutral atoms, but in applied catalysis, the catalyst precursor most often consists of ions and counterions. Only in the final stage of the preparation, catalyst precursors are reduced to neutral atoms, and only when the metallic phase is the active phase. In other cases, catalyst nanoparticles are ionic compounds throughout their lifetime. Hence, for studying nanoparticle

Received: July 2, 2019
Published: July 22, 2019

formation during the preparation of applied catalysts and for studying sintering during application of unreduced catalysts, the diffusion of metal ions over hydroxylated surfaces needs to be studied and not that of neutral atoms.

Especially on "active" supports, such as γ-alumina, many ions tend to bind in an isolated fashion over the surface, meaning that they initially do not take part in nanoparticles but are ligated by the surface hydroxylation layer, which isolates the cations from each other.[33] Often, such cations carry additional hydration, even at chemical potentials of water at which the surface starts to dehydrate.[34] Understanding and controlling the diffusion of ions on such surfaces may be the next step for improving the accuracy of catalyst preparation. To the best of our knowledge, the diffusion of ions on hydroxylated oxide surfaces has not been modeled yet. With respect to the experimental research, we did find one case study,[35,36] but experimentally, it is very difficult to recognize the mechanistic intricacies of ion diffusion.

Here, we study the diffusion of copper ions over hydroxylated γ-alumina, specifically over the (110) surface. $CuCl_2$ on γ-Al_2O_3 is used as a catalyst for oxychlorination of ethylene into 1,2-dichloroethane, an intermediate in the production of poly(vinyl chloride).[37,38] For this catalyst, the active phase is the ionic state, so understanding and controlling the diffusion behavior of the copper ions are useful both for the preparation and for the stability upon application. For this catalyst, we studied previously the OH coordination and hydration of Cu^{2+} at varying chemical potentials of water, recognized as varying hydroxylation states of the surface.[34] In the current paper, we focus on the diffusion of the (hydrated) copper ions in this system and how this is affected by changing circumstances.

Our main goal is elucidation of potential diffusion mechanisms and factors controlling them by comparing energy barriers. Note that for translating these barriers to actual diffusion coefficients, also kinetic prefactors would need to be determined.[39] We are especially interested in the effects of valence state, counterions, and hydroxylation levels since these may present handles to improve control. Hence, we study the diffusion behavior of Cu^{2+} and Cu^{+}, with and without Cl^{-} counterions, at varying hydroxylation levels of the γ-alumina surface. We will show how the diffusion behavior of metal ions is strongly dependent on how the moving charge is compensated, either by codiffusion of counterions or contra-diffusion of protons.

METHODS

All calculations were performed with the SIESTA code (version 3.2),[40,41] interfaced via the ASE suite,[42] using the revised Perdew–Burke–Enzerhof (rPBE) functional.[43] Improved Troullier–Martins pseudopotentials[44] with relativistic corrections were used using input parameters from the Octopus project.[45] For aluminum and copper, core corrections were applied with pseudocore radii of 0.92 and 0.84 bohr, respectively. Basis sets of three different qualities were used: default SZ and DZP basis sets and a specially optimized TZP (and TZ2P for aluminum) basis set, as optimized previously,[46] combined with density mesh cutoffs of 70 Ry (for SZ and DZP) and 100 Ry (for TZ(2)P). In all cases, a 2-fold grid-cell sampling was added and the electronic structure was converged to 10^{-3} eV. All calculations containing Cu^{2+} were performed in the spin state $S = 1/2$. Since all systems are overall neutral, no background charge was needed.

When charged species move over an hydroxylated surface, it is important that the surface structure adjusts itself to the moving charge. However, many types of adjustments, e.g., proton jumps, do not occur during simple minimization procedures. Moreover, since many variations are possible, it is infeasible to systematically study all possibilities, as infeasible as performing full molecular dynamics (MD) simulations at the high-quality density functional theory level for this type of system. Hence, we pull the Cu ion in different directions with steps of 0.2 Å, while at every step, we perform very short explorative MD simulations[47] at high temperature to allow the OH groups to move and adjust. Then, from several points in these MD simulations, the structure is optimized and the energy is compared to the energy of the optimized structure before the MD simulations. The structure with the lowest energy is selected for the next step. Note that during the MD simulations and all optimizations, one coordinate of the diffusing Cu ion is constrained, while all other degrees of freedom are kept free to move (except for one Al atom in the bulk to anchor the system). At each point in the curve, three MD simulations with random starting velocities were started of 1000 MD steps each and optimizations were performed after 500 and 1000 steps, resulting in six alternative structures.

All optimizations were performed at DZP level, with the Broydon–Fletcher–Goldfarb–Shanno optimizer,[48] and were converged to 0.05 eV/Å. The explorative MD simulations were performed at the SZ level since they are only needed for low-quality sampling. In these simulations, the temperature was set to 600 K and time steps of 0.3 fs were used. For increased sampling efficiency, the weights of the atoms were lowered to 2 u for O and 4 u for Cu and Cl.

Figure 1 compares the energy barriers for Cu^{2+} diffusion in one direction in a test system (the (110) surface with five H_2O per unit cell, but constructed slightly differently than the structures used for the production runs), modeled with and without the explorative MD simulations. Without additional sampling, the barriers are seriously overestimated and the

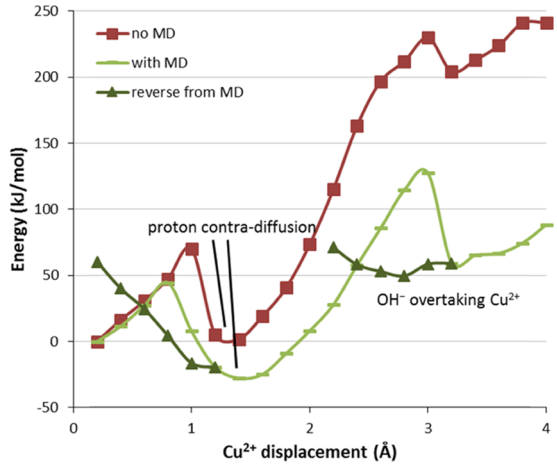

Figure 1. Energy barriers for Cu^{2+} diffusion in a test system with five H_2O per unit cell, modeled with and without explorative MD. When the Cu ion is pulled while only optimizing all other coordinates (red curve), the second surface adjustment (codiffusion of OH^{-}) is missed. Using explorative MD at each step (light green curve) brings down the barrier significantly. Adding a reverse series (dark green curve) gives the likely true path when at the crossing point of the curves the paths are connected via NEB calculations.

DOI: 10.1021/acs.jpcc.9b06291
J. Phys. Chem. C 2019, 123, 18502–18507

critical surface adjustment (a long distance OH displacement) is missed. Our sampling procedure does find correct structure adjustments but still tends to overestimate the barriers since adjustments often are not yet found until the energy gain is large enough. Therefore, from each minimum in the curves, reverse pulls are also performed (with only minimizations), and from the crossing points of the curves, the actual diffusion barriers are calculated with the nudged elastic band (NEB) method.[49,50] At selected points on the forward and backward curves, unconstrained reoptimizations are performed and used as start and end points for the NEB calculations.

The NEB calculations were performed at the DZP level with 10 images (including start and end points). The most efficient convergence was obtained when using the FIRE optimizer and a NEB string constant of 0.01 eV/Å^2. First, a nonclimbing-image, run was performed (using the "aseneb" option), followed by climbing-image NEB (combined with the "elastic-band" option) to find the true transition state, both converged to 0.08 eV/Å. Typically, convergence was obtained in 200−400 steps in total. Finally, for each system, the lowest barrier was selected and all barriers within 50 kJ/mol were recalculated with the TZ(2)P basis set, starting from the converged DZP results. In some cases, convergence of the high-quality NEB calculations was troublesome. These were redone using 15 NEB images. Since the quantitative accuracy of the resulting diffusion barriers turned out to be limited, we refrained from further characterizing the transition states with frequency calculations.

The γ-alumina surface model of Digne et al. was used.[24,51,52] The structure of Cu^{2+} on the γ-alumina (110) surface at maximum hydroxylation (6 H_2O = 12 OH per unit cell plus one additional H_2O on the Cu^{2+} ion) was taken from our previous work, in which it was constructed by replacing two protons with one Cu^{2+} ion.[34] In the x and y directions, one additional unit cell with six water molecules but without copper was added. The thickness of the slab was halved, resulting in a layer thickness of 8 Å and a total of 234 atoms in the periodic supercell. To prevent bias against deep-lying diffusion paths, we did not freeze the bottom layers of the slab. This led to a small relaxation, bringing some oxygen atoms in the bottom layer more toward the bottom surface, with atomic movements of up to 0.5 Å. For later quantitative studies, freezing of the bottom layers may need to be reconsidered. The total supercell dimension (including vacuum in the z direction) was 16.18 × 17.38 × 25.0 Å^3.

In ref 34, we compared lowest energy structures at each hydroxylation state, assuming thermodynamic equilibration. However, for the current work, systematic series are needed in which the Cu is still at the original position. Hence, all starting structures were constructed accordingly by sampling removal of the most likely OH groups and protons, followed by six explorative MD runs in each case. Similarly, structures with Cu^+ (readding one proton to the Cu^{2+} system and resampling removal of water molecules) and additional Cl^- (replacing 1 OH^-) were constructed from the same starting point, followed by explorative MD runs again. In some cases with Cu^+, during modeling of the diffusion barriers, sampling resulted in structures with even lower energies. When the difference was more than 20 kJ/mol, calculations were restarted with these structures as new starting points.

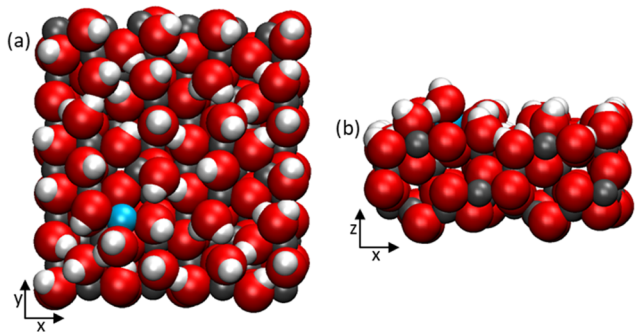

Figure 2. Top (a) and side (b) views of Cu^{2+} on the fully hydroxylated γ-Al_2O_3(110) surface with six H_2O (12 OH) per unit cell and one Cu^{2+} per supercell. This structure was copied from ref 34 and adapted to a supercell of 2 × 2 × 0.5 unit cell.

RESULTS

The starting structure of Cu^{2+} on the fully hydroxylated γ-Al_2O_3(110) surface is depicted in Figure 2. This structure was used as a starting point for all other structures, which are shown in Figures S1−S3. From these starting points, the Cu ion was pulled in four different directions, the energy profiles of which are shown in Figure S4a−k. The results for Cu^{2+} with four H_2O per unit cell are shown in Figure 3.

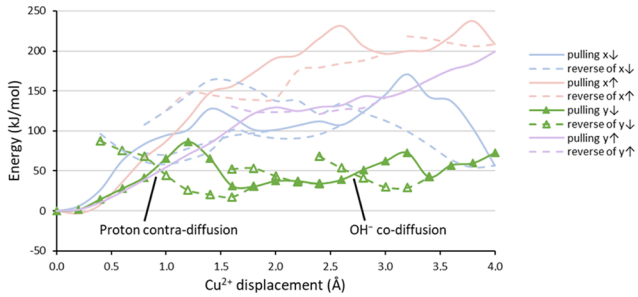

Figure 3. Energy profiles for diffusion in four directions of Cu^{2+} over the γ-Al_2O_3(110) surface with four H_2O per unit cell. The path with the lowest barriers is shown with a bright color; the colors of the other curves remain pale. The Cu^{2+} ion was pulled in four alternative directions: in positive (↑) or negative (↓) direction along the x-axis or the y-axis. Reverse series (pulling the Cu^{2+} back toward its original x or y coordinate) are shown with open symbols. In this system, two mechanisms occur: proton contradiffusion and OH^- codiffusion. For both steps, the final barrier as calculated with the NEB method is around 110 kJ/mol.

While all paths and energy profiles are rather different from each other, it is clear that whenever the Cu ion is forced to move the energy goes up significantly until the surface structure adjusts itself and the energy decreases again. Apparently, the copper ions cannot move smoothly in between or over the surface hydroxyl groups, but their movement is critically dependent on the behavior of these hydroxyl groups. In retrospect, this is very logical since it is charged species that are moving. Without surface adjustments, a charge separation would occur between the cation and its counterions. However, since the OH^- ions are strongly bound to the surface and to each other, the energy needed to let charge compensations occur determines the diffusion barrier for the Cu cation. Interestingly, in many cases, charge compensation does not occur only by counterion codiffusion, but we also observe many instances of proton contradiffusion, which is an

DOI: 10.1021/acs.jpcc.9b06291
J. Phys. Chem. C 2019, 123, 18502−18507

alternative way to compensate cation movement. In principle, codiffusion of two OH^- ions is also possible, but this leads to roughly twice as high barriers, so this was not observed in any case.

By selecting the lowest pathway for each structure, the resulting diffusion barriers from the NEB calculations are shown in Figure 4. However, when rerunning a few points with

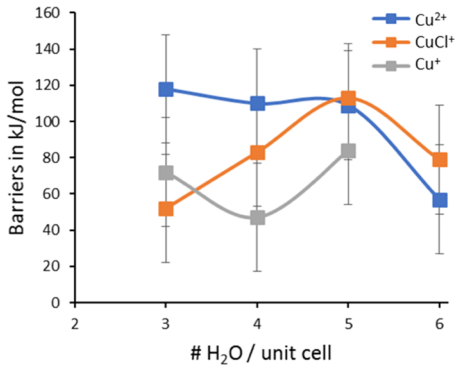

Figure 4. Lowest diffusion barriers for Cu^{2+}, $CuCl^+$, and Cu^+ over the γ-Al_2O_3(110) surface at varying hydration states, as found using the DZP basis set. The quantitative values should be handled with care, though.

15 NEB images instead of 10, and recalculating most energies with the TZ(2)P basis set, a very large spread in energies (up to 60 kJ/mol) was found. Therefore, the quantitative value of these results is rather limited and should be handled with care. Nevertheless, qualitatively, some very interesting observations can be made that make sense mechanistically: at 3, 4, and 5 H_2O per unit cell, the diffusion barriers for Cu^{2+} are relatively high since codiffusion of OH^- is difficult. In these cases, a combination of limited proton contradiffusion and OH^- codiffusion is observed. At full hydroxylation, however, the hydrogen bond network is fully connected and proton contradiffusion over longer distances occurs and no OH^- codiffusion is observed (Figure 5).

When a Cl^- counterion is added (by exchanging it for an OH^-), the counterion can more easily follow the Cu^{2+} ion and the Cu^{2+} diffusion barrier is lowered. Interestingly, the bonding of the chloride varies for different hydroxylation states, which is reflected in the diffusion barriers for Cu^{2+}: at full hydroxylation, the chloride sits on top of the copper and

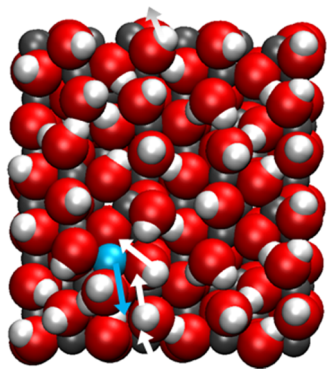

Figure 5. Proton contradiffusion during the diffusion of Cu^{2+} over the γ-Al_2O_3(110) surface with maximum hydroxylation (six H_2O per unit cell). In this case, the Cu^{2+} moves underneath the H_2O molecule.

follows very easily. At lower hydroxylation, however, the chloride interacts directly with an aluminum atom and diffusion barriers increase accordingly. When the hydroxylation state becomes even lower, the Cu^{2+} ion starts to lack neighbors and the Cl^- binds stronger to Cu, thereby weakening its interaction with Al. As a result, the $CuCl^+$ pair can now diffuse more easily again. The interactions of the Cl with Cu and Al can be recognized from its distance to these atoms (Table 1).

Table 1. Cl−Cu and Cl−Al Distances, in Å, as a Function of Hydroxylation Level[a]

# H_2O per unit cell	Cl−Cu distance	Cl−Al distance
6	2.25	4.20
5	2.21	2.55
4	2.22	2.51
3	2.14	3.37

[a]At the lowest hydroxylation level, the Cl−Al interaction weakens because the Cu^{2+} claims the Cl^-.

Finally, Cu^+ tends to behave differently than Cu^{2+}: for Cu^+, hardly any charge compensation is observed, but the Cu^+ diffuses as a lone ion, with only local adjustments of the surface structure. In this case, increased hydroxylation levels tend to hinder Cu^+ diffusion slightly as protons tend to be in the way of the copper ion and are sometime pushed deeper into the surface while Cu^+ passes by. It is worth mentioning also for Cu^{2+} that when counting the number of codiffusing or contradiffusing species, the charge is only compensated partially in our periodic models. When diffusion over longer distances is considered or of multiple cations moving in the same direction, more charge compensation may need to occur, but this cannot be studied with the current model.

DISCUSSION

Our methodology proved effective for finding qualitatively unknown pathways, without causing any bias. However, obtaining full sampling in this way is rather costly. Also, it was found that automated quantitative analysis of the barrier heights using NEB calculations is problematic for the complex pathways that were obtained. Therefore, for further quantitative analysis, we advise a systematic study of the elementary steps of the obtained mechanisms using more directed sampling strategies.

Although current quantitative accuracy is limited, we have found some clear trends for the mechanisms with which the Cu ions are diffusing. For Cu^{2+}, charge compensation is critical for allowing any diffusion, which can happen either via OH^- codiffusion or proton contradiffusion or both. When the hydrogen bond network of the surface hydroxyl groups is fully connected, full proton contradiffusion is possible and the diffusion barriers for Cu^{2+} diffusion are low. However, when the hydrogen bond network is not fully connected, the possibilities for proton contradiffusion are limited to a short range and the Cu^{2+} diffusion depends on counterion codiffusion. In that case, the barriers for cation diffusion depend mostly on the bonding strength of the counterions to the surface, either due to hydrogen bonds from the other OH groups or due to direct interaction with the Al atoms. Note that any direct binding of Cu^{2+} to the surface is much weaker than the binding of the counterions to the surface.

Based on this, we can postulate some trends that can be expected for cation diffusion on hydroxylated surfaces in

DOI: 10.1021/acs.jpcc.9b06291
J. Phys. Chem. C 2019, 123, 18502−18507

general. First of all, since charge compensation is critical, diffusion barriers for cations are likely related to their valence state. However, when the hydrogen bond network of the surface hydroxyl groups is fully connected, these barriers decrease significantly because the needed charge compensation can then be completely covered by proton contradiffusion. In practice, though, out of all typical catalyst supports we expect that this is only the case for γ-alumina at high humidity. For any other support, surface hydroxylation is not of such level that the hydrogen bond network is fully connected.

With respect to the counterion codiffusion, the rule that the bonding strength of the counterion to the surface controls the diffusion barriers for both cation and counterions will likely be a general rule as well. Hence, one can expect that surfaces that bind surface hydroxyl groups only weakly will allow cations to diffuse easier. On the other hand, for γ-alumina, one may expect that the addition of halogen counterions will improve the diffusion of any cation. However, also for any cation, complications will exist with respect to variations in the hydroxylation state since the bonding of the halogens to the surface also varies with the hydroxylation state.

Finally, for reducible oxide surfaces, we expect the trends in cation diffusion to be different because on such surfaces charge compensation can occur through the bulk material.

CONCLUSIONS

For the first time, the diffusion of charged species over a hydroxylated surface has been modeled. It was found that the key issue for diffusion of charged species is compensation of the moving charge, which can occur either by proton contradiffusion or by counterion codiffusion.

On the modeling side, it was found that explorative MD can be used for this type of system, delivering efficient sampling. However, for successful quantitative analysis of the barriers using automated NEB calculations, the variations in the possible pathways were too complicated. Now that we have identified the main mechanistic tendencies, a more systematic study of the elementary steps is desirable. Nevertheless, we did identify interesting trends and mechanistic insights regarding the effects of valency, hydroxylation level, and counterion identity on the diffusion of cations on hydroxylated surfaces. We expect this will open new leads for control in the preparation of solid catalysts and similar materials.

ASSOCIATED CONTENT

Supporting Information

The Supporting Information is available free of charge on the ACS Publications website at DOI: 10.1021/acs.jpcc.9b06291.

Starting structures and energy profiles for the ion diffusion in four directions of Cu^{2+}, $CuCl^{+}$, and Cu^{+} over the γ-Al_2O_3(110) surface with 3–6 H_2O per unit cell (PDF)

AUTHOR INFORMATION

Corresponding Author

*E-mail: m.j.louwerse@hetnet.nl.

ORCID

Manuel J. Louwerse: 0000-0003-4847-2536

Notes

The authors declare no competing financial interest.

ACKNOWLEDGMENTS

This work has been supported by the Dutch Topsector Chemie through the project CHEMIE.PGT.2016.006 "Modeling Ion Diffusion during Preparation to Improve Catalyst Selectivity (MIDPICS)". We acknowledge usage of the Dutch national supercomputer Cartesius as funded by NWO as part of the projects SH-273-15 and SH-273-16.

REFERENCES

(1) Satterfield, C. N. *Mass Transfer in Heterogeneous Catalysis*; MIT Press: Massachusetts, 1970.

(2) van den Berg, R.; Elkjaer, C. F.; Gommes, C. J.; Chorkendorff, I.; Sehested, J.; de Jongh, P. E.; de Jong, K. P.; Helveg, S. Revealing the Formation of Copper Nanoparticles from a Homogeneous Solid Precursor by Electron Microscopy. *J. Am. Chem. Soc.* **2016**, *138*, 3433–3442.

(3) Narayanan, R.; El-Sayed, M. A. Effect of Catalysis on the Stability of Metallic Nanoparticles: Suzuki Reaction Catalyzed by PVP-Palladium Nanoparticles. *J. Am. Chem. Soc.* **2003**, *125*, 8340–8347.

(4) Prieto, G.; Zečević, J.; Friedrich, H.; de Jong, K. P.; de Jongh, P. E. Towards Stable Catalysts by Controlling Collective Properties of Supported Metal Nanoparticles. *Nat. Mater.* **2013**, *12*, 34–39.

(5) Ala-Nissila, T.; Ferrando, R.; Ying, S. C. Collective and Single Particle Diffusion on Surfaces. *Adv. Phys.* **2002**, *51*, 949–1078.

(6) Tsong, T. T. Mechanisms and Energetic of Atomic Processes in Surface Diffusion. *Physica A* **2005**, *357*, 250–281.

(7) Ehrlich, G. Diffusion of Individual Adatoms. *Surf. Sci.* **1994**, *299/300*, 628–642.

(8) Kellogg, G. L. Field Ion Microscope Studies of Single-Atom Surface Diffusion and Cluster Nucleation on Metal Surfaces. *Surf. Sci. Rep.* **1994**, *21*, 1–88.

(9) Perkins, L. S.; DePristo, A. E. Self-Diffusion Mechanisms for Adatoms on fcc(100) Surfaces. *Surf. Sci.* **1993**, *294*, 67–77.

(10) Liu, C. L.; Cohen, J. M.; Adams, J. B.; Voter, A. F. EAM Study of Surface Self-Diffusion of Single Adatoms of fcc Metals Ni, Cu, Al, Ag, Au, Pd, and Pt. *Surf. Sci.* **1991**, *253*, 334–344.

(11) Hansen, L.; Stoltze, P.; Jacobsen, K. W.; Nørskov, J. K. Self-Diffusion on Copper Surfaces. *Phys. Rev. B* **1991**, *44*, 6523–6526.

(12) Feibelman, P. J. Diffusion Path for an Al Adatom on Al(001). *Phys. Rev. Lett.* **1990**, *65*, 729–732.

(13) Feibehnan, P. J. A Novel Tool for Surface Electronic Structure Calculations—Insight into Surface Self-Diffusion on Metals. *Adv. Mater.* **1992**, *4*, 396–401.

(14) Stumpf, R.; Scheffler, M. Ab Initio Calculations of Energies and Self-Diffusion on Flat and Stepped Surfaces of Al and Their Implications on Crystal Growth. *Phys. Rev. B* **1996**, *53*, 4958–4973.

(15) Barcaro, G.; Fortunelli, A.; Nita, F.; Ferrando, R. Diffusion of Palladium Clusters on Magnesium Oxide. *Phys. Rev. Lett.* **2005**, *95*, No. 246103.

(16) Xu, L. J.; Henkelman, G.; Campbell, C. T.; Jónsson, H. Pd Diffusion on MgO(100): The Role of Defects and Small Cluster Mobility. *Surf. Sci.* **2006**, *600*, 1351–1362.

(17) Šljivančanin, Ž. Collective Diffusion of Gold Clusters and F-Centers at MgO(100) and CaO(100) Surfaces. *J. Phys. Chem. C* **2014**, *118*, 28720–28724.

(18) Negreiros, F. R.; Fabris, S. Role of Cluster Morphology in the Dynamics and Reactivity of Subnanometer Pt Clusters Supported on Ceria Surfaces. *J. Phys. Chem. C* **2014**, *118*, 21014–21020.

(19) Jeon, J.; Yu, B. D. Dynamics of Pd Monomers and Dimers Adsorbed on the (001) Surfaces of Strongly Correlated Nickel Oxides. *Curr. Appl. Phys.* **2015**, *15*, 98–102.

(20) Haas, G.; Menck, A.; Brune, H.; Barth, J. V.; Venables, J. A.; Kern, K. Nucleation and Growth of Supported Clusters at Defect Sites: Pd/MgO(001). *Phys. Rev. B* **2000**, *61*, 11105–11108.

(21) Sterrer, M.; Risse, T.; Giordano, L.; Heyde, M.; Nilius, N.; Rust, H.-P.; Pacchioni, G.; Freund, H.-J. Palladium Monomers,

Dimers, and Trimers on the MgO(001) Surface Viewed Individually. *Angew. Chem., Int. Ed.* **2007**, *46*, 8703−8706.
(22) Łodziana, Z.; Nørskov, J. K.; Stoltze, P. The Stability of the Hydroxylated (0001) Surface of α-Al_2O_3. *J. Chem. Phys.* **2003**, *118*, 11179−11188.
(23) Briquet, L. G. V.; Catlow, C. R. A.; French, S. A. Platinum Group Metal Adsorption on Clean and Hydroxylated Corundum Surfaces. *J. Phys. Chem. C* **2009**, *113*, 16747−16756.
(24) Digne, M.; Sautet, P.; Raybaud, P.; Euzen, P.; Toulhoat, H. Use of DFT to Achieve a Rational Understanding of Acid−Basic Properties of γ-Alumina Surfaces. *J. Catal.* **2004**, *226*, 54−68.
(25) Zhuravlev, L. T. The Surface Chemistry of Amorphous Silica. Zhuravlev model. *Colloids Surf., A* **2000**, *173*, 1−38.
(26) Addou, R.; Senftle, T. P.; O'Connor, N.; Janik, M. J.; van Duin, A. C. T.; Batzill, M. Influence of Hydroxyls on Pd Atom Mobility and Clustering on Rutile TiO_2(011)-2 × 1. *ACS Nano* **2014**, *8*, 6321−6333.
(27) Corral Valero, M.; Raybaud, P.; Sautet, P. Influence of the Hydroxylation of γ-Al_2O_3 Surfaces on the Stability and Diffusion of Single Pd Atoms: a DFT Study. *J. Phys. Chem. B* **2006**, *110*, 1759−1767.
(28) Meyer, R.; Ge, Q. F.; Lockemeyer, J.; Yeates, R.; Lemanski, M.; Reinalda, D.; Neurock, M. An Ab Initio Analysis of Adsorption and Diffusion of Silver Atoms on Alumina Surfaces. *Surf. Sci.* **2007**, *601*, 134−145.
(29) Tosoni, S.; Pacchioni, G. Influence of Surface Hydroxylation on the Ru Atom Diffusion on the ZrO_2(101) Surface: a DFT Study. *Surf. Sci.* **2017**, *664*, 87−94.
(30) Heemeier, M.; Stempel, S.; Shaikhutdinov, S. K.; Libuda, J.; Bäumer, M.; Oldman, R. J.; Jackson, S. D.; Freund, H.-J. On the Thermal Stability of Metal Particles Supported on a Thin Alumina Film. *Surf. Sci.* **2003**, *523*, 103−110.
(31) Pomp, S.; Kaden, W. E.; Sterrer, M.; Freund, H.-J. Exploring Pd Adsorption, Diffusion, Permeation, and Nucleation on Bilayer SiO_2/Ru as a Function of Hydroxylation and Precursor Environment: From UHV to Catalyst Preparation. *Surf. Sci.* **2016**, *652*, 286−293.
(32) Munnik, P.; de Jongh, P. E.; de Jong, K. P. Recent Developments in the Synthesis of Supported Catalysts. *Chem. Rev.* **2015**, *115*, 6687−6718.
(33) Leofanti, G.; Padovan, M.; Garilli, M.; Carmello, D.; Zecchina, A.; Spoto, G.; Bordiga, S.; Turnes Palomino, G.; Lamberti, C. Alumina-Supported Copper Chloride: 1. Characterization of Freshly Prepared Catalyst. *J. Catal.* **2000**, *189*, 91−104.
(34) Louwerse, M. J.; Rothenberg, G. Modeling Catalyst Preparation: The Structure of Impregnated−Dried Copper Chloride on γ-Alumina at Low Loadings. *ACS Catal.* **2013**, *3*, 1545−1554.
(35) Wang, H.-F.; Ariga, H.; Dowler, R.; Sterrer, M.; Freund, H.-J. Surface Science Approach to Catalyst Preparation − Pd Deposition onto Thin Fe_3O_4(111) Films From $PdCl_2$ Precursor. *J. Catal.* **2012**, *286*, 1−5.
(36) Sterrer, M.; Freund, H.-J. Towards Realistic Surface Science Models of Heterogeneous Catalysts: Influence of Support Hydroxylation and Catalyst Preparation Method. *Catal. Lett.* **2013**, *143*, 375−385.
(37) Lamberti, C.; Prestipino, C.; Bonino, F.; Capello, L.; Bordiga, S.; Spoto, G.; Zecchina, A.; Diaz Moreno, S.; Cremaschi, B.; Garilli, M.; et al. The Chemistry of the Oxychlorination Catalyst: an In Situ, Time-Resolved XANES Study. *Angew. Chem., Int. Ed.* **2002**, *41*, 2341−2344.
(38) Muddada, N. B.; Fuglerud, T.; Lamberti, C.; Olsbye, U. Tuning the Activity and Selectivity of $CuCl_2$/γ-Al_2O_3 Ethene Oxychlorination Catalyst by Selective Promotion. *Top. Catal.* **2014**, *57*, 741−756.
(39) Bolhuis, P. G.; Chandler, D.; Dellago, C.; Geissler, P. L. Transition Path Sampling: Throwing Ropes over Rough Mountain Passes, in the Dark. *Annu. Rev. Phys. Chem.* **2002**, *53*, 291−318.
(40) Ordejón, P.; Artacho, E.; Soler, J. M. Self-Consistent Order-N Density-Functional Calculations for Very Large Systems. *Phys. Rev. B* **1996**, *53*, R10441−10444.
(41) Soler, J. M.; Artacho, E.; Gale, J. D.; García, A.; Junquera, J.; Ordejón, P.; Sánchez-Portal, D. The SIESTA Method for Ab Initio Order-N Materials Simulation. *J. Phys.: Condens. Matter* **2002**, *14*, 2745−2779.
(42) Larsen, A. H.; Mortensen, J. J.; Blomqvist, J.; Castelli, I. E.; Christensen, R.; Dulak, M.; Friis, J.; Groves, M. N.; Hammer, B.; Hargus, C.; et al. The Atomic Simulation Environment—a Python Library for Working with Atoms. *J. Phys.: Condens. Matter* **2017**, *29*, No. 273002.
(43) Hammer, B.; Hansen, L. B.; Nørskov, J. K. Improved Adsorption Energetics within Density-Functional Theory using Revised Perdew-Burke-Ernzerhof Functionals. *Phys. Rev. B* **1999**, *59*, 7413−7421.
(44) Troullier, N.; Martins, J. L. Efficient Pseudopotentials for Plane-Wave Calculations. *Phys. Rev. B* **1991**, *43*, 1993−2006.
(45) Octopus Pseudopotential Generator. 2010, http://www.tddft.org/programs/octopus/pseudo.php (accessed Oct 1, 2010).
(46) Louwerse, M. J.; Rothenberg, G. Transferable Basis Sets of Numerical Atomic Orbitals. *Phys. Rev. B* **2012**, *85*, No. 035108.
(47) Mager-Maury, C.; Bonnard, G.; Chizallet, C.; Sautet, P.; Raybaud, P. H_2-Induced Reconstruction of Supported Pt Clusters: Metal−Support Interaction versus Surface Hydride. *ChemCatChem* **2011**, *3*, 200−207.
(48) Shanno, D. F. Conditioning of Quasi-Newton Methods for Function Minimization. *Math. Comput.* **1970**, *24*, 647−656.
(49) Henkelman, G.; Jónsson, H. Improved Tangent Estimate in the Nudged Elastic Band Method for Finding Minimum Energy Paths and Saddle Points. *J. Chem. Phys.* **2000**, *113*, 9978−9985.
(50) Henkelman, G.; Uberuaga, B. P.; Jónsson, H. A Climbing Image Nudged Elastic Band Method for Finding Saddle Points and Minimum Energy Paths. *J. Chem. Phys.* **2000**, *113*, 9901−9904.
(51) Digne, M.; Sautet, P.; Raybaud, P.; Euzen, P.; Toulhoat, H. Hydroxyl Groups on γ-Alumina Surfaces: a DFT Study. *J. Catal.* **2002**, *211*, 1−5.
(52) Krokidis, X.; Raybaud, P.; Gobichon, A.-E.; Rebours, B.; Euzen, P.; Toulhoat, H. Theoretical Study of the Dehydration Process of Boehmite to γ-Alumina. *J. Phys. Chem. B* **2001**, *105*, 5121−5130.

DOI: 10.1021/acs.jpcc.9b06291
J. Phys. Chem. C 2019, 123, 18502−18507